Remote Sensing and Wavelet Analysis for 30 Year Non-linear Non-stationary Teleconnection Signal Identification Between Sea Surface Temperature and Precipitation Regime in Central America

Miguel Valdez Vasquez [1], and Chi-Farn Chen [1,2]
[1] Department of Civil Engineering, National Central University,
Jhongli City, Taoyuan 32001, Taiwan
[2] Center for Space and Remote Sensing Research, National Central University,
Jhongli City, Taoyuan 32001, Taiwan

ABSTRACT. The effect that Sea Surface Temperature (SST) has on vegetation dynamics and precipitation throughout the world has been demonstrated widely. SST variations have been linearly linked with greenness and precipitation through ocean-atmospheric interactions such as El Nino Southern Oscillation (ENSO), North Atlantic Oscillation (NAO), Pacific Decadal Oscillations (PDO) and Atlantic Multi-Decadal Oscillations (**AMO**) among others. Previous research has demonstrated that teleconnection can be used for climate prediction across a wide region at sub-continental scales. Although these studies are very important, the results are more difficult to interpret as linear analyses were used only to examine these relationships. In this paper 30-year, non-stationary signals are identified between SST at the Atlantic and Pacific oceans, and precipitation in the La Amistad International Park at Panama, Central America. The site was selected to avoid noise that can cause biased results. The methodology proposed for the teleconnection pattern identification has 3 major steps. First, the pre-processing of data, which involves the detrending by estimating the anomaly for the terrestrial and oceanic datasets. Furthermore, linear analysis was performed to the anomaly data in order to identify statistically significant regions of correlation between SST and the terrestrial site's precipitation. Indexes are selected in the regions of significant correlation. A second filter is applied by using a Stepwise Regression analysis to identify the most influential ocean regions. Finally, Wavelet analysis is used for the identification of non-stationary signals among the terrestrial dataset anomaly and SST anomaly. It was found that throughout the ocean regions there has been a link with ENSO, and during low ENSO years, with the NAO via atmospheric circulations. Also a link is found with the AMO and PDO. High frequency signals are also displayed in the time series which may coincide with the seasonal variations. These identified long-term teleconnection signals can aid for understanding the climate change impacts at local scales, and can aid to determine precipitation forecasts by establishing a relationship in the information identified.

Keyword: SST, Precipitation, Wavelet, ENSO, NAO.

1. INTRODUCTION

Central America is a particular land surrounded by the Pacific and Atlantic Oceans, and two continental land masses, North and South America (CCAD-SICA, 2010). In addition, the region has a very strong climate distinction between the humid and rainy Caribbean region, which is very vulnerable to large floods because of its intense rainfalls and the dry Pacific coast which is prone to drought and has a long intense dry season. An analysis of climate extremes in Central America during 1961–2003 indicated an increase in extreme warm maximum and minimum temperatures, rainfall events, and contribution of wet and very wet days (Aguilar et al., 2005). An effect of this is majorly on vegetation greenness, as observed in the rainforests of Brazil in which forests have been replaced by grasslands (Barbosa, 2006; Papadopoulos, 2009). Variability in rainfall events was predicted as the main climate change factor in tropical forests (Harshthorn, 1992); hence, forest composition and greenness are affected by drought patterns in areas with sharp precipitation gradients such as those in Central America (Condit, 1998).

Precipitation, as previously stated, plays an important role in vegetation dynamics in this region, and a pattern modification as a result of the rise of Sea Surface Temperature (SST) can cause more frequency of the extreme climate events (Papadopoulos, 2009). Precipitation is also one of the most important climatic variables that has been associated to ocean atmospheric patterns (Lovejoy, 2005).

How climate change are affecting precipitation regime locally is still an important task for academics worldwide, until now, significant progress has been made (Aguilar et al., 2005; Barbosa, 2006; Cho et al., 2010; Huber & Fensholt, 2011; Keener et al., 2010).

The most widely known ocean atmospheric pattern which causes interannual variability is the El Niño-Southern Oscillation (ENSO) (Shabbar, 2006), which has been often linked with the Central American region (Magaña et al., 2003; Mason & Goddard, 2001). In Central America, the impacts of ENSO on precipitation regime, air temperature, and vegetation dynamics were highlighted in several previous studies (Ropelewski and Halpert,

1987; George, 1998; Chiew and Mcmahon, 2002; Karmalkar et al., 2011) Other studies however not only direct to ENSO as a main driver of local variability(Hagemeyer, 2006; Waylen et al., 1998).In addition (Dettinger et al., 2001; Muñoz et al., 2010; Alfaro and Cortés, 2012) relate the occurrence of cold fronts in Central America to the North Atlantic Oscillation (NAO) and found a relationship between the Pacific–North America (PNA) teleconnection pattern with climate anomalies of the Intra-Americas Sea (i.e. Gulf of Mexico and Caribbean Sea).

Previous research also studied the impacts of interaction of teleconnection patterns on local precipitation in Central America and found that extremely dry periods in Costa Rica are linked with the PNA and NAO during neutral or low ENSO conditions (Waylen et al., 1998; Alfaro and Cortés, 2012).

To understand the climate change effects on precipitation and its interannual, biennial, triennial to multidecadal inconsistency tackles a great degree of importance, therefore the topic recently gained relevance (Hodson et al., 2009). Some other important findings include the association found between the Atlantic Ocean and Amazonian greenness, showing a strong correlation between NDVI and SST in certain regions of the Amazon and the Atlantic Ocean (Cho et al., 2010). Preceding studies examined the major source of interannual and interdecadal climate variability of ENSO, NAO, and PNA and evaluated the impact of these large-scale climate phenomena on precipitation and other climatic variables in Central America (Dettinger et al., 2001; Aguilar et al., 2005; Karmalkar et al., 2011; Alfaro and Cortés, 2012). However, few articles have been issued to report the likely influences of non-leading teleconnection patterns, which are not related to the known climate teleconnections, on local meteorology in this unique Central America region.

The objectives of this study thus, were to explore coherency among precipitation and teleconnection patterns based on 30 year anomaly SST and precipitation time series, and explore the impacts on the terrestrial precipitation. La Amistad International Park in Panama was selected as the study area. To do the study, linear correlation is applied to anomaly SST-Precipitation to find regions that have a strong statistical significance. Furthermore, wavelet analysis is used to identify discrete biennial-triennial significant signal which may indicate a link or an effect of the oceanic SST on the terrestrial response. The results acquired can be of great importance for future projections of local terrestrial variables and its responses to climate change effects and may be used to forecast the most relevant climatic variables based on non-linear and non-stationary teleconnection signals.

2. STUDY AREA

La Amistad International Park is located in the Talamanca mountain range, which rises from near sea level to more than 3800m. The park was selected for the study because it is considered to be the largest virgin forest in Panama. Wildfire was historically not a common natural disturbance within the park, and tropical cyclones do not have a direct impact. The Panama sector of La Amistad International Park is located in the western region of the country and has a total territorial extension of 207 000 ha (Figure 1). In addition, the oceanic study region selected are the regions of Pacific and Atlantic oceans which include major phenomena such as ENSO, NAO, PNA and Atlantic Multi-decadal oscillation (AMO) as well as Pacific Decadal Oscillation (PDO).

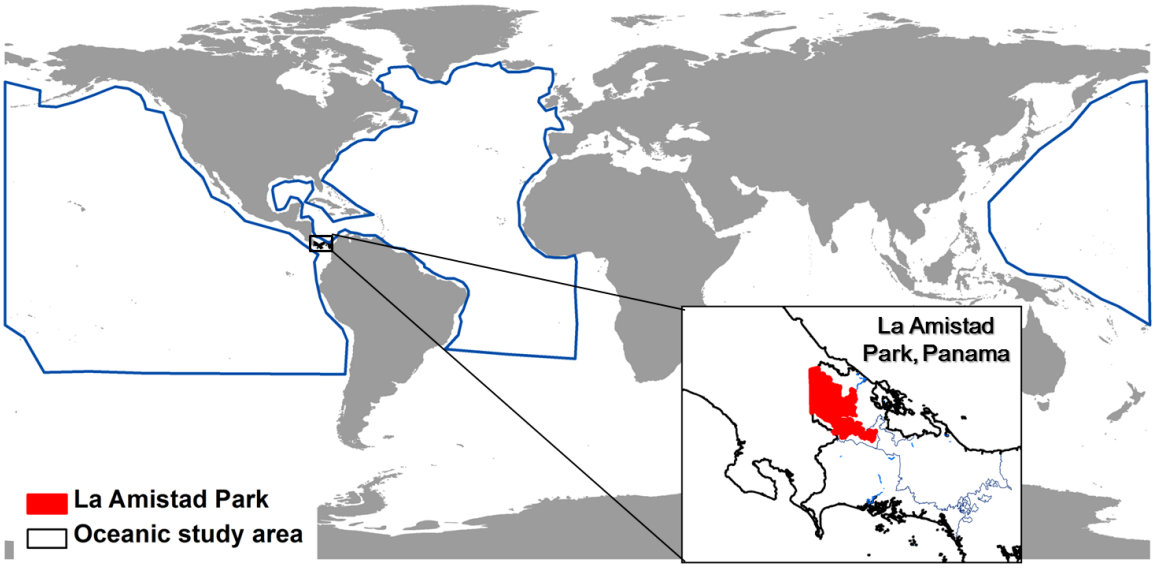

Figure 1. Oceanic region: Atlantic and Pacific Oceans. Terrestrial site: La Amistad Park, Panama

3. MATERIALS AND METHODS

The methodology initially emphasizes in selecting an adequate study area and pre-processing data-sets acquired from different sensors to then follow up with three major sub steps (Figure 2). Each of the sub-steps followed are described in detail.

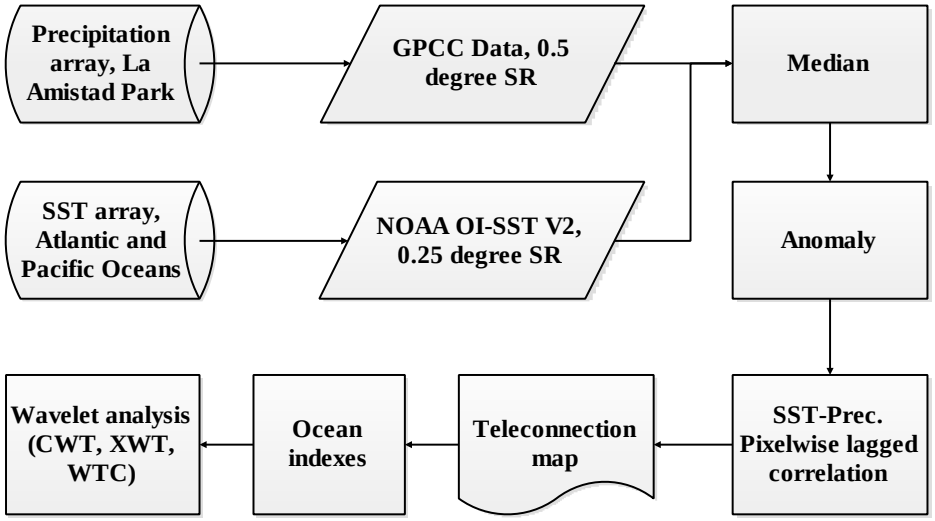

Figure 2. Analytical framework of the study

3.1 Data acquisition and pre-processing

Three types of data are used in this study: The NOAA Optimum Interpolation SST Version 2 (NOAA OI SST V2) High Resolution Dataset which was acquired from the NOAA High-resolution Blended Analysis and provides SST data on a daily basis with a spatial resolution of 0.25 degrees which was then resampled to 0.5 degrees for faster computation**.** For precipitation the GPCC Global Precipitation Climatology Centre monthly precipitation dataset was used with a spatial resolution of 0.5 degrees and has a daily coverage. Precipitation was converted to monthly totals. Anomaly was estimated for both time series in order to remove seasonality.

3.2 Linear analysis

3.2.1 Pixelwise linear lagged correlation analysis: For the linear correlation analysis we used the pixel wised Pearson correlation coefficient for all the grids of Precipitation-SST. The equation to estimate is as follows:

$$r = \left(\frac{\sum_i^n [(x_i - \mu(x)) * (y_{i-d} - \mu(y)])}{\sqrt{\sum_i^n (x_i - \mu(x))^2} \times \sqrt{\sum_i^n (y_{i-d} - \mu(y))^2}} \right) \quad \textbf{(1)}$$

Where *r* is the correlation coefficient, *n* is the number of values in a time series, *x* is a terrestrial time series, *y* is the SST time series, μ is the mean of a time series, and *d* is the time lag. The correlation coefficient is applied to the datasets and correlation maps estimated using 0 to 12 months' time lags.

3.3 Wavelet Analysis

A wavelet analysis was applied to quantify and visualize statistically significant changes in monthly Atlantic and Pacific SST and the terrestrial EVI as well as precipitation over the pristine forested site. Specifically, three types of wavelet analysis, namely continuous wavelet transform (CWT), cross wavelet transform (XWT), and wavelet coherence (WTC), were applied in this study.

3.3.1 Continuous Wavelet Transform

The CWT is a type of wavelet transform which is particularly useful for feature extraction purposes. (Keener et al., 2010). A wavelet is a function with zero mean and that is localized in both frequency and time. We can characterize a wavelet by how localized it is in time and frequency. The Morlet wavelet is used in this study, which is a wavelet consisting of a plane wave modulated by a Gaussian:

$$\psi(\eta) = \pi^{0.25}\, e^{i\omega\eta} e^{-0.5\eta^2} \quad \textbf{(2)}$$

Where is the no dimensional frequency. Morlet wavelets are non-orthogonal, complex functions that can be used with the continuous wavelet transform *Wn (s)*. The advantage of the Morlet wavelet over other candidates such as the Mexican hat wavelet resides in its good definition in the spectral space . The idea behind the CWT is to apply the wavelet as a band pass filter to the time series. The wavelet is stretched in time by varying its scale (s), so that _=s•t, and normalizing it to have unit energy. The continuous wavelet transform W_n of a discrete sequence of observations X_n is defined as the convolution of X_n with a scaled and translated wavelet ψ(η) that depends on a nondimensional time parameter η, and is given by:

$$W_n^x(S) = \sum_{n'=0}^{N-1} X_{n'}\, \psi^* \left[\frac{(n'-n)\delta t}{s}\right] \quad \textbf{(3)}$$

Where *n* is the localized time index, *s* is the wavelet scale, δt is the sampling period, *N* is the number of points in the time series, η' is the translated time index, ψ is the normalized wavelet and the asterisk indicates the complex conjugate.
An approximate value of W_n can be found by performing the convolution N times for each scale, where N is the number of points in the time series. All convolutions can then be done in Fourier space using a discrete Fourier transform of xn, (Eq.(3)), which is:

$$\hat{x}_k = \left(\frac{1}{N}\right) \sum_{n=0}^{N-1} x_n\, exp^{-2\pi ikn/N} \quad \textbf{(4)}$$

where $k = 0, \ldots, N-1$ is the frequency index. By the convolution theorem, the wavelet transform is the inverse Fourier transform of the product of the discrete Fourier transform of xn and ψ*, with angular frequency ω_k:

$$(S) = \sum_{k=0}^{N-1} \hat{X}_k \hat{\psi}^*(s\omega_k) exp^{i\omega_k n\delta t} \quad \textbf{(5)}$$

Finally, the wavelet power spectrum is defined as $|W_n(s)|^2$ and the amplitude at each point $|W_n(s)|$ and phase can be found.

3.3.2 Cross Wavelet Transform

Cross Wavelet Transform (XWT) is performed in this study to find regions in time frequency space where the time series show high common power, therefore, significance. XWT particularly, studies whether regions in time frequency space with large common power have a consistent phase relationship, which suggests teleconnection between the time series (Grinsted, Moore, & Jevrejeva, 2004). Given two time series X and Y the XWT is defined as:

$$W_n^{XY}(s) = W_n^X(s)\, W_n^{Y*}(s) \quad \textbf{(6)}$$

Where (*) denotes the complex conjugate. The cross wavelet power can be defined as $|W_n^{XY}(s)|$.

3.3.3 Wavelet Coherency

Computing the wavelet-coherence transform (WTC) finds regions in time frequency space where the two time series co-vary, but do not necessarily have high power. For this reason, both are necessary when analyzing two time series to assess both causality and local co-variance. The wavelet-coherence transform of two time series is defined as:

$$R_n^2(s) = \frac{\left|S(s^{-1}W_n^{XY}(s))\right|^2}{S\left(s^{-1}\left|S\left(W_n^X(s)\right)\right|^2\right)\cdot S(s^{-1}\left|S(W_n^Y(s))\right|^2} \quad \textbf{(7)}$$

Where *S* is a smoothing operator defined by the wavelet type used and the entire expression is similar to that of a traditional correlation coefficient localized in time frequency space. The statistical significance level of the wavelet coherence is estimated using Monte Carlo methods, and the significance level for each scale is calculated using only values outside the cone-of-influence.

4. RESULTS AND DISCUSSION

4.1 Linear analysis

From the linear analysis we aim to identify the regions in the Pacific and Atlantic Oceans that showed statistically significant positive and negative correlation with the terrestrial dataset. After performing the Pearson's lagged linear correlation analysis to the anomaly data of each terrestrial site, the results mapped (Figure 3) show that a strong correlation exists in large regions throughout the Atlantic and Pacific oceans. We can observe a very clear positively significant correlation between ENSO region and the precipitation in the terrestrial study site that slowly drifts from El Nino 3 to El Nino 1+2 regions. NAO and PNA also present statistically significant correlation in the later lags. From this regions identified, indexes were extracted to further analyze (Figure 4). The indexes extracted were all related to major oceanic patterns as shown in Table 1.

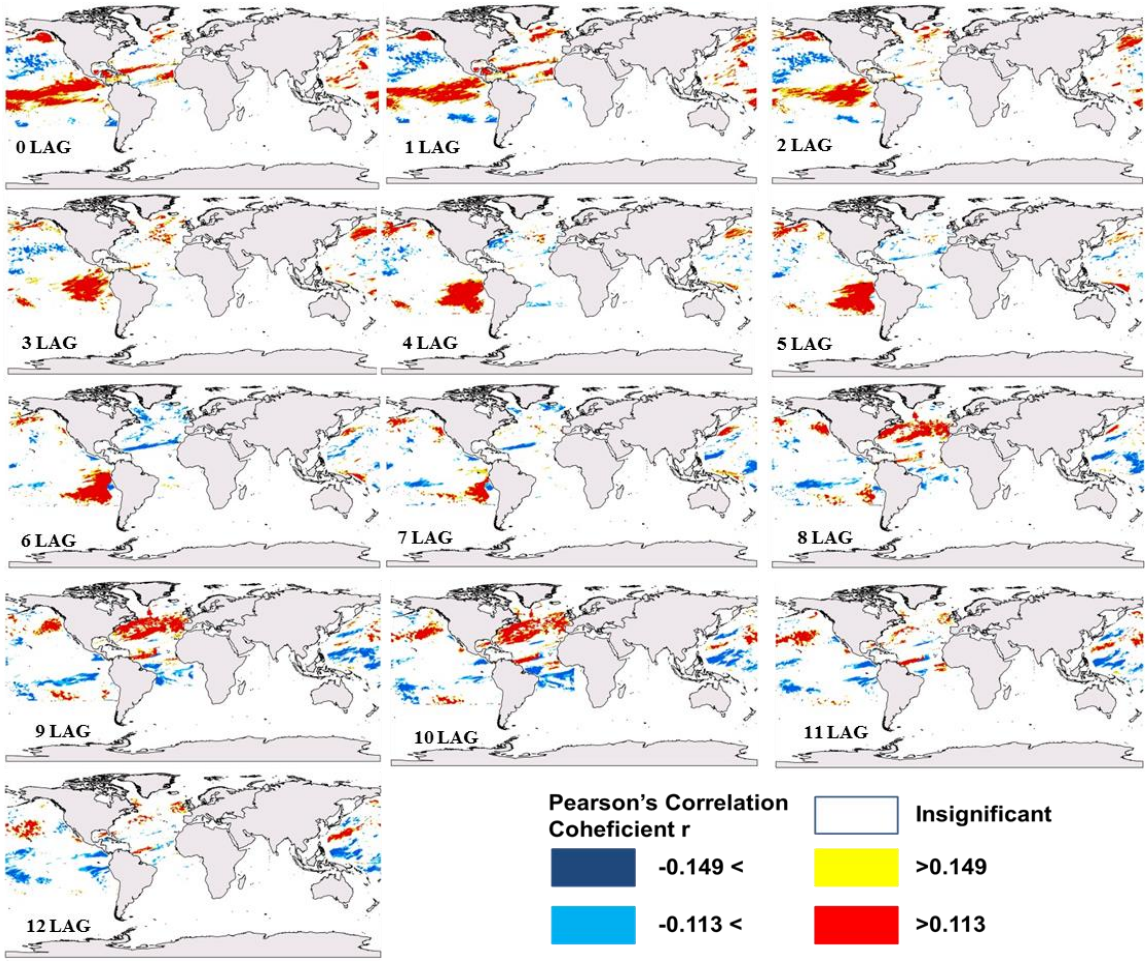

Figure 3. Linear correlation maps for SST-Precipitation. Red and yellow represent statistically significant regions of correlation at the 99% and 95% confidence level respectively. Blue and light blue represent statistically significant regions of anti-correlation at the 99% and 95% confidence level respectively.

Table 1. Indexes selected and its relation with ocean-atmospheric patterns

Oceanic Index	Index 1	Index 2	Index 3	Index 4	Index 5	Index 6	Index 7
NAO				X	X		
ENSO	X	X					X
PNA			X				X
PDO							
AMO						X	

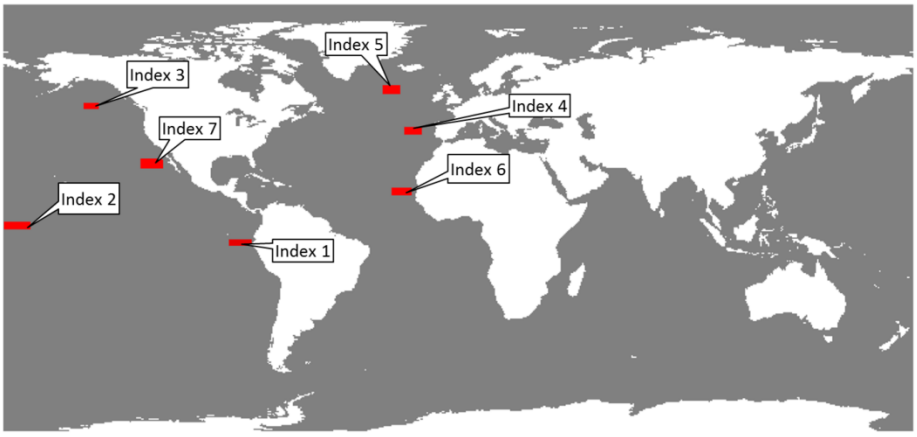

Figure 4. Indexes selected in oceanic regions that have high correlation with precipitation in terrestrial site.

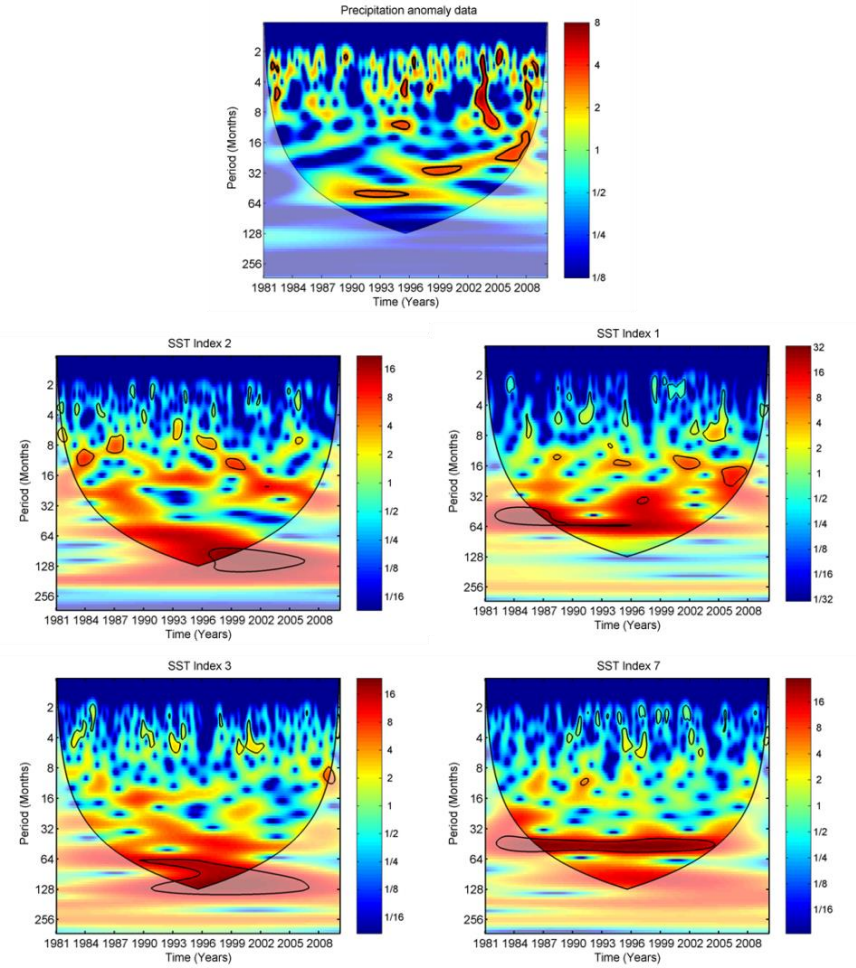

Figure 5. CWT of Precipitation and SST Indexes.

4.2 Wavelet Analysis

Based on the results of the linear correlation analysis and indices selected, CWT, XWT and WTC images are provided (Figure 5 and 6). This analysis can provide a more significant understanding of which periods and moment of the time series, high common power and covariation is observed. It can give us an indication of a link between the SST variations and the precipitation on the terrestrial site. The CWT image expands the one-dimensional time series into a two-dimensional time-frequency figure. The XWT analysis measures high common power shared by the two time series.

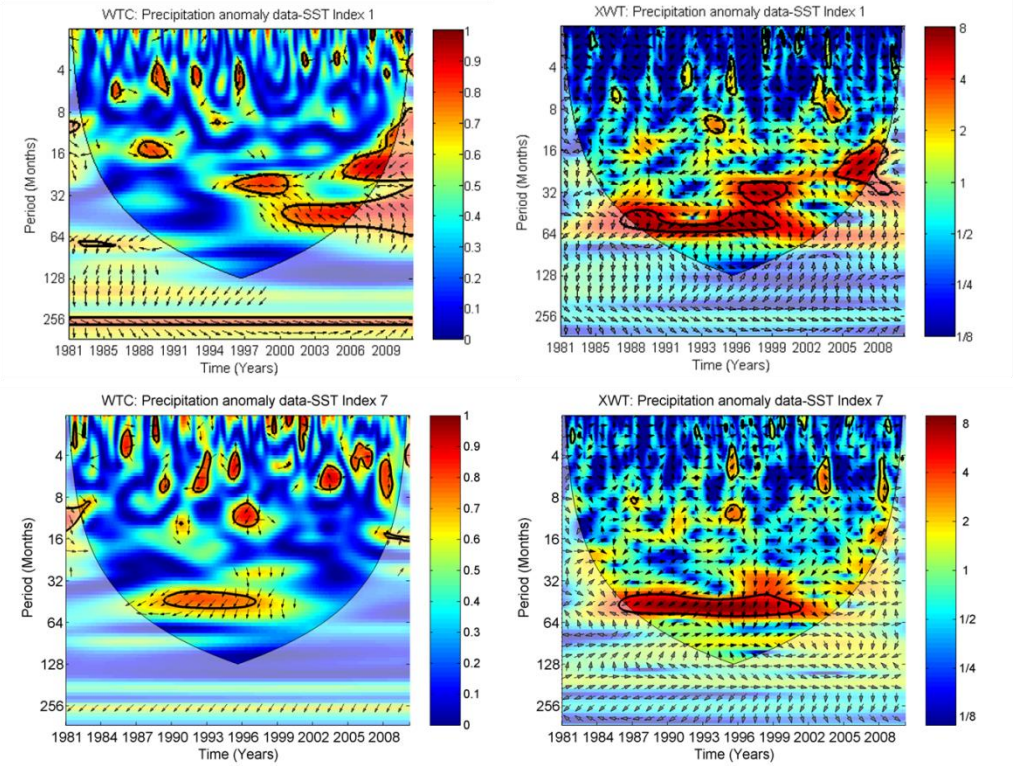

Figure 6. WTC and XWT for: SST Index 1-Precipitation in terrestrial site time series and SST Index 7-Precipitation in terrestrial site time series.

WTC shows where two time series locally co-vary but do not necessarily have high common power. WTC is performed to show coherency between time series datasets. The XWT and WTC also images illustrate phase arrows which determine phase direction and lead/lag relationships. (Figure 6). Arrows pointing to the right indicate that the two time series are in-phase, whereas arrows pointing to the left indicate the anti-phase relationship. Arrows pointing up indicate that SST is leading precipitation. Areas within the black bold lines indicate 95% confidence level with red indicating high power and blue indicating low power.

From the results acquired for CWT in the high frequency domain (2-12 month period) it can be observed significant power regions scattered throughout the whole time series. This may represent the seasonality changes in the region. In the lower frequency periods, between 16-32 month period, also significant regions are found between 1993-1995 and 1997-1999 and 2005. The SST indexes CWT also show similar significant regions of low frequency signals however with a more extended period (32-128 month period).

From XWT between SST index 1 and precipitation, a strong low frequency signal is observed in the 32-64 month period starting in 1988 until 1999 which coincides with El Nino events occurred between those years and with drought condition records. Then a weak signal is observed in the 16 months period between 2005-2008. For the results acquired, SST leads precipitation. Strong linkage between the El Nino region 1+2 and the precipitation dynamics in the terrestrial site is observed and both time series are negatively correlated. The WTC also show in similar periods and times, strong coherency between both datasets time series, in the16-64 month period extending itself from 2005 until the end of the time series. The XWT and WTC for SST index 7 show a low frequency signal between the 32-64 month period which extends itself from 1984 until 2000. This index region is related to the lower region of PNA. The results indicate a linkage between extreme ENSO conditions and the times in which strong coherency between SST and precipitation is shown.

5. CONCLUSIONS

In this study, combined remote sensing and wavelet analysis are used to identify climate teleconnection signals between SST and vegetation/precipitation of a protected area in Panama, Central America. In order to identify which regions of Atlantic and Pacific oceans may have a stationary link with terrestrial variable, pixelwise linear lagged correlation analysis was applied. Regions which have a constant statistical significant correlations among datasets are selected as indices to further analyse them using wavelet analysis for the detection of non-stationary signal. The results obtained indicate an interannual high frequency signal and biennial to triennial low-frequency signal between SST anomalies and precipitation anomalies in the Atlantic and Pacific Oceans. The strong coherency shown between the El Nino 1+2 region with the precipitation during the high ENSO conditions is in

accordance with several studies developed previously. In addition, its anti-phase relationship coincides with drought reports in Panama during certain times of our time series. Further analysis and experimentation is required to enrich the results acquired.

6. REFERENCES

Aguilar, E., Peterson, T. C., Obando, P. R., Frutos, R., Retana, J. A., Solera, M., Soley, J., et al. (2005). Changes in precipitation and temperature extremes in Central America and northern South America, 1961–2003. *Journal of Geophysical Research*, *110*(D23107), 1–15. doi:10.1029/2005JD006119

Alfaro, E. J., & Cortés, J. (2012). Atmospheric forcing of cool subsurface water events in Bahía Culebra , Gulf of Papagayo , Costa Rica. *Revista Biologica Tropical [online]*, *60*(2), 173–186.

Barbosa, H. (2006). Interannual Variability of Vegetation Dynamics In The Semi-Arid Northeast Region of Brazil And Its Relationship to Enso Events. *International Conference on Southern Hemisphere Meteorology and Oceanography* (pp. 855–860). Iguacu, Brazil. Retrieved from http://onlinelibrary.wiley.com/doi/10.1002/cbdv.200490137/abstract

CCAD-SICA. (2010). Problematic and Impact of the Climate Change Variability on the Region. In R. Rodriguez (Ed.), *Regional Strategy on Climate Change, 2012* (p. 95). San Salvador: Comision Centroamericana para el Desarollo, Sistema de Integracion Centroamericana.

Cho, J., Yeh, P., Lee, Y., Kim, H., Oki, T., Kanae, S., Kim, W., et al. (2010). A study on the relationship between Atlantic sea surface temperature and Amazonian greenness. *Ecological Informatics*, *5*(5), 367–378. doi:10.1016/j.ecoinf.2010.05.005

Dettinger M.D., Battisti D.S., Bitz C.M., (2001). Interhemispheric effects of interannual and decadal ENSO-like climate variations on the Americas. In Interhemispheric Climate Linkages, Markgraf V (ed). Academic Press: San Diego, CA; 454.

Hagemeyer, B. (2006). The Relationship Between ENSO, PNA, and AO/NAO and Extreme Storminess, Rainfall, and Temperature Variability During the Florida Dry Season: Thoughts on Predictability and Attribution. *Proceedings of 18th Conference on Climate Variability and Change, American Meteorologial Society* (p. 16). Atlanta, Georgia.

Harshthorn G.S., (1992). Forest loss and future options in Central America, Hagan JM III, Johnston DW (eds). In Ecology and conservation of neotropical migrant land birds, Smithsonian Institution Press: Washington, D.C.; 13–22.

Huber, S., & Fensholt, R. (2011). Analysis of teleconnections between AVHRR-based sea surface temperature and vegetation productivity in the semi-arid Sahel. *Remote Sensing of Environment*, *115*(12), 3276–3285. doi:10.1016/j.rse.2011.07.011

Karmalkar, A. V., Bradley, R. S., & Diaz, H. F. (2011). Climate change in Central America and Mexico: regional climate model validation and climate change projections. *Climate Dynamics*, *37*(3-4), 605–629. doi:10.1007/s00382-011-1099-9

Keener, V. W., Feyereisen, G. W., Lall, U., Jones, J. W., Bosch, D. D., & Lowrance, R. (2010). El-Niño/Southern Oscillation (ENSO) influences on monthly NO3 load and concentration, stream flow and precipitation in the Little River Watershed, Tifton, Georgia (GA). *Journal of Hydrology*, *381*(3-4), 352–363. doi:10.1016/j.jhydrol.2009.12.008

Lovejoy, T. (2005). Climate change and biodiversity. *Rev. sci. tech. Off. int. Epiz.*, *27*(2), 1–8.

Magaña, V. O., Vázquez, J. L., Pérez, J. L., & Pérez, J. B. (2003). Impact of El Niño on precipitation in Mexico. *Geofisica Internacional*, *42*(3), 313–330.

Mudelsee, M. (2003). Estimating Pearson's Correlation Coefficient with Bootstrap Confidence Interval from Serially Dependent Time Series. *Mathematical Geology*, *35*(6), 651–665. doi:10.1023/B:MATG.0000002982.52104.02

Papadopoulos, B. T. (2009). *Climate Change in Latin America*. (B. T. Papadopoulos, Ed.) (p. 110). Lima, Peru: European Commision.

Poveda, G., & Mesa, O. (1997). Feedbacks between Hydrological Processes in Tropical South America and Large-Scale Ocean – Atmospheric Phenomena. *Journal of Climate*, *10*(10), 2690–2702.

Shabbar, A. (2006). The impact of El Nino-Southern Oscillation on the Canadian climate. *Advances in Geoscience*, *6*, 149–153.

Waylen, P., Caviedes, C., Poveda, G., Mesa, O., & Quesada, M. (1998). Rainfall Distribution and Regime in Costa Rica and its Response to the El Nino-Southern Oscillation.pdf. *Yearbook, Conference of Latin Americanists Geographers*, *24*, 75–84.